International Journal on Future Revolution in Computer Science & Communication Engineering
Volume: 4 Issue: 5
ISSN: 2454-4248
36 – 47

Color Image Enhancement via Combine Homomorphic Ratio and Histogram Equalization Approaches: Using Underwater Images as Illustrative Examples

Artyom M. Grigoryan
Department of Electrical and Computer Engineering
University of Texas at San Antonio
San Antonio, TX 78249-0669
amgrigoryan@utsa.edu

Sos S. Agaian
Computer Science Department
The College of Staten Island
New York, USA
Sos.Agaian@csi.cuny.edu

***Abstract*—**The histogram is one of the important characteristics of grayscale images, and the histogram equalization is effective method of image enhancement. When processing color images in models, such as the RGB model, the histogram equalization can be applied for each color component and, then, a new color image is composed from processed components. This is a traditional way of processing color images, which does not preserve the existent relation or correlation between colors at each pixel. In this work, a new model of color image enhancement is proposed, by preserving the ratios of colors at all pixels after processing the image. This model is described for the color histogram equalization (HE) and examples of application on color images are given. Our preliminary results show that the application of the model with the HE can be effectively used for enhancing color images, including underwater images. Intensive computer simulations show that for single underwater image enhancement, the presented method increases the image contrast and brightness and indicates a good natural appearance and relatively genuine color.

***Keywords* —** *Image enhancement, histogram equalization, color models, color enhancement measure.*

*****

I. INTRODUCTION

Image enhancement and image resolution are very crucial in many remote sensing image processing applications, such as hyper-spectral data feature extraction [1], classification[2,6] and segmentation [3,7], cloud detection [4,5], remote sensing measurements [8,9]. However, the low remote sensing image resolution and image quality limits above applications [9].

In the last few decades, underwater image analytics has become an active research area in ocean engineering [10]-[17]. The image quality of underwater images plays a key role in many practical underwater imaging systems that include the monitoring of sea life, marine ecological research, accessing geological environment, aquatic robot inspection of the underwater cables and pipelines, underwater photography, and ocean search and rescue [18,19]. Therefore, effective methods to enhance and analyze underwater images are very important and desired [20]. The existing image analytics research, which includes image enhancement, shows that underwater images advance new challenges and carry out major engineering problems because of (a) the physical properties of underwater environment which causes the degradation of the images; (b) the absorption and scattering effects of the water that limit the visibility of underwater objects resulting images captured by underwater cameras, which are usually suffered from a low contrast, non-uniform illumination, blurring, bright artifacts, noise, and diminished color [11,12]; (c) it is hard to acquire visible agreeable images due to the absorptive and dispersion nature of sea water; (d) the visibility of the image is inadequate in the underwater environment (the image colors can be washed out in a distance around 12m in clear water, and almost 5m in turbid water [24]); (e) insufficient research in analysis of underwater images. As a result, degraded underwater images show some limitations when being used in above applications and decrease the accuracy rate of underwater object detection and segmentation, and marine biology recognition [19,20].

The image enhancement is a powerful tool for many image processing applications, including the underwater imaging, wherein it is required to improve characteristics and quality of images, especially color images [31,32],[58]-[60],[77,78]. Many image enhancement algorithms have been developed for processing grayscale images that are based on the human visual system and, then, applied to color images. The existent methods of color image enhancement can be divided by three classes (see the review in [76]). The first two classes process color images, by using the traditional approach; i.e., the color components of the images are processed separately. This approach to color image enhancement cannot always adaptively compensate the contrast degradation of underwater images and new methods should be developed for restoring colors and enhancing contrast of underwater images. Here, we can separate the methods which enhance color image components directly in the spatial domain into the first class, and methods developed in the frequency domain belong to the second class. The first class includes many methods using different look-up tables, which include the square-root and log transformations [73], unsharp masking [22],[68], histogram equalization [28], histogram modification techniques [21]-[27],[30,34,35], monotonic sequences [29], contrast masking [24] and contrast entropy [69,71].

 ISSN: 2454-4248
36 – 47

The second class of methods is with unitary transforms, such as the Fourier, Hartley, Hadamard, heap, and cosine transforms [38]-[44],[66]-[70],[84]. Among these transforms, the discrete Fourier transform (DFT) plays the most important role in grayscale image enhancement [37,58,59]. In this class of methods, we can mention the method of alpha-rooting and its modifications that include the alpha-rooting by zones, which are simple and effective when processing grayscale images [33,38,54,59,30]. The tensor transform allows for processing and enhancing the image by direction image components [53],[55]-[57]. The retinex method with different modifications [72]-[76] can also be included in this class, since the fast realization of the multi-scale retinex with the Gaussian filters is performed through the DFT.

Recently, several high quality image enhancements have been developed, by transferring color images from different color models to quaternion space [46] and, then, processing by the two-dimensional quaternion Fourier transform (2-D QDFT) [47],[79]-[83]. We refer these methods to the third class of color image enhancement methods. In color-to-quaternion images, the color at each pixel is considered and processed as one unit. Due to fast algorithms of the 2-D QDFTs [48,49], transform-based methods of image enhancement can effectively used for color imaging that can be considered as a part of the quaternion imaging. Here, we mention the method of alpha-rooting of color image enhancement by the 2-D left-side, right-side, and two-side QDFTs [45,51,52], as well as the method of color enhancing through the enhancing direction color image components in tensor representation [49,50].

As illustration of methods of the above mentioned three classes of image enhancement, we consider the color image “Ancuti3 input.jpg” from [78]. Figure 1 shows this image of size 768×1024 in part (a), the histogram equalization performed on each color component of the image in part (b), the component-wise alpha-rooting by the 2-D DFT in part (c). The red, green, and blue components were processed with α=0.80, 0.84, and 0.78, respectively. The alpha-rooting of the color image, by the 2-D quaternion DFT and α = 0.70, is shown in part (d).

Figure 1. (a) The original image in the RGB color mode, (b) component-wise HE, (c) component-wise (0.80,0.84,0.78)-rooting by the 2-D DFTs, and (d) the 70-rooting by the 2-D QDFT.

In this paper, we introduce a novel approach to color image enhancement that is not referred to any of the three major classifications of the existing image enhancement methods that were mentioned above. A new model for color image processing is proposed when the color image is represented by a grayscale image and the ratios of the color components at each pixel are calculated and used later after enhancing the grayscale image, in order to reconstruct the colors from the new grays. This model is simple and can be used for any color model, including the RGB, XYZ, and HSV color spaces [28,46]. In this model, the method of histogram equalization is applied. This process is called the color histogram equalization and illustrated on different color images. The quality of the color image enhancement is estimated by the well-known measure EMEC [45]-[47]. The rest of the paper is organized in the following way. Section 2 presents the diagram and the main steps of the new model for color image processing. The measure of color image enhancement, EMEC, is also described. The application of the color histogram equalization is described in detail in Section 3. Examples of color image enhancement by the HE in the proposed model are given. Section 4 describes the application of the bi-HE in the proposed model with examples. Conclusion is in Section 5.

II. MODELS WITH COLOR RATIOS

In this section, a new approach for color image enhancement is described, by transforming color images into gray-scales, applying the known method of histogram equalization (HE) with subsequent composition of new color images, by using the ratios of color components in original color images. The enhancement is described for images in the RBG color model; other color models, such as the XYZ, CMY(K), and many others, can similarly be used.

The distinguishing feature of the proposed model over the existing models can be described as follows: (1) the color components at each pixel are processed as one unit, not separate; (2) only one grayscale image is processed; and (3) the characteristics of colors are preserving. Here, the characteristics are related to the color ratios at each pixel, such as red/green and red/blue, and green/blue ratios. These characteristics can be described by the ratios of the red, green, and blue colors to the gray. The block-diagram of the proposed color histogram equalization (CHE) in the RGB color model is shown in Fig. 2.

 ISSN: 2454-4248
36 – 47

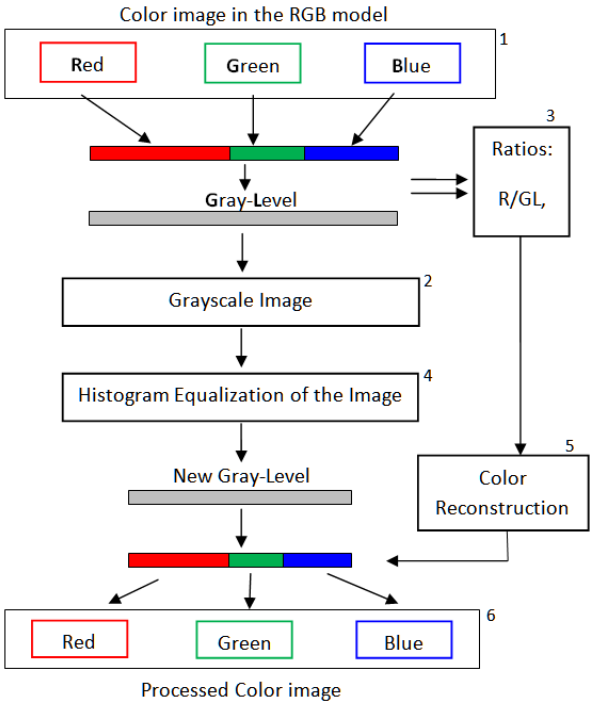

Figure 2. Block-diagram of color image HE.

This block-diagram has the following main steps:

Step 1 (block 1): The color image

$$f_{n,m} = (r_{n,m}, g_{n,m}, b_{n,m})$$

of size $N \times M \times 3$ is presented as three channel image with primary color components, r(ed), g(reen), and b(lue) in pixels in the RGB model.

Step 2 (block 2): The color image $f_{n,m}$ is transferring to the grays, by using one of the compositions of type

$$i_{n,m} = a_1 r_{n,m} + a_2 g_{n,m} + (1 - a_1 - a_2) b_{n,m}. \quad (1)$$

Here, values of parameters a_{21} and a_2 are selected from the interval (0,1). For instance, the case when $a_2 = a_1 = 1/3$is for the grayscale image

$$i_{n,m} = (r_{n,m} + g_{n,m} + b_{n,m})/3, \quad (2)$$

and the case when $a_1 = 0.3$ and $a_2 = 0.59$ is for the grayscale image of brightness,

$$i_{n,m} = 0.3 r_{n,m} + 0.59 g_{n,m} + 0.11 b_{n,m}. \quad (3)$$

Step 3 (block 3): Two ratios of the colors are calculated at each pixel by

$$\lambda_1 = \lambda_1(n,m) = r_{n,m}/(r_{n,m} + g_{n,m} + b_{n,m}) \quad (4)$$

and

$$\lambda_2 = \lambda_2(n,m) = \frac{g_{n,m}}{r_{n,m} + g_{n,m} + b_{n,m}}, \quad (5)$$

if we select the red and green colors. Then, the similar ratio for the blue color can be calculated by $(1 - \lambda_1 - \lambda_2)$.

The color ratios can also be calculated as $\lambda_3 = \lambda_3(n,m) = g_{n,m}/r_{n,m}$ and $\lambda_4 = \lambda_4(n,m) = b_{n,m}/r_{n,m}$, or any other two ratios between three colors. In this case, $\lambda_1 = 1/(1 + \lambda_1 + \lambda_2)$, and $\lambda_2 = \lambda_1 \lambda_3$.

Step 4 (block 4): The grayscale image is processed by the histogram equalization,

$$i_{n,m} \to i'_{n,m}. \quad (6)$$

Step 5 (block 5): It is assumed that the new image represents the color image in the same model, i.e.,

$$i'_{n,m} = a_1 r'_{n,m} + a_2 g'_{n,m} + (1 - a_1 - a_2) b'_{n,m}. \quad (7)$$

Therefore, the colors can be calculated from the grays $i'_{n,m}$ of the processed image, by using the color ratios calculated in Step 3; namely,

$$\begin{aligned} r'_{n,m} &= \lambda_1 s'_{n,m} \\ g'_{n,m} &= \lambda_2 s'_{n,m} \\ b'_{n,m} &= (1 + \lambda_1 + \lambda_2) s'_{n,m} = s'_{n,m} - r'_{n,m} - g'_{n,m}, \end{aligned} \quad (8)$$

where the sum of new colors $s'_{n,m} = r'_{n,m} + g'_{n,m} + b'_{n,m}$ can be calculated by

$$s'_{n,m} = \frac{i'_{n,m}}{a_1\lambda_1 + a_2\lambda_2 + (1 - a_1 - a_2)(1 - \lambda_1 - \lambda_2)}. \quad (9)$$

Step 6 (block 6): The new color image in the RGB model is calculated by

$$f'_{n,m} = (r'_{n,m}, g'_{n,m}, b'_{n,m}). \quad (10)$$

A. Histogram Equalization and Color Ratios

The histogram is one of the important characteristics of grayscale images. The histogram is a function $h(r)$ defined on the integer range $[0, L]$ of the discrete image $g_{n,m}$ of size $N \times M$. This function at each point r gives the number [cardinality (card)] of pixels (n,m) in the image with the level r of intensity, $h(r) = card\{(n,m);\ g_{n,m} = r\}$. The values of r are in the range of intensities $[r_0, r_1]$, where $r_0 = \min(f)$ and $r_1 = \max(f)$. The histogram is normalized as $h(r) = h(r)/N/M$, so that $0 < h(r) < 1$. In the HE, the monotonic transformation is used

$$T(r) = T(r_0) + [T(r_1) - T(r_0)]F(r), \quad (11)$$

where the discrete distribution function of intensity is calculated as

$$F(r) = h(r_0) + h(r_0 + 1) + \cdots + h(r), r = r_0 : r_1.$$

For many images, the range of intensities is the integer interval [0,255]. In this case, the transform in Eq. 11 has a simple form: $T(r) = 255F(r)$ being rounding to integer. The HE is based on the idea of transforming the image into another image with the histogram having equal values.

 ISSN: 2454-4248
36 – 47

Theoretically, the equalization can be achieved on a 2-D function $f(x,y)$ on the plane, but not on discrete images gn,m, which are defined on a discrete lattice and have quantized values. Therefore, the HE as a look-up table (with the scaled cumulative density function) when applied for the discrete image $g_{n,m}$ results in an image with a histogram that is more flat than the original histogram.

The conventional HE tends to change the mean brightness of the image to the middle level of the dynamic range by leaving too much empty space on the grayscale and results in annoying artifacts and intensity saturation effects and the noises of the whole image are also increased. To solve this problem, several new techniques, including mean brightness preserving histogram equalization, have been proposed [25]-[27],[60]. All above methods of HE cannot directly be applied to color images because of modifying the relationship between original color image components (red, green, and blue). To reconstruct image component relationship, a several color correction algorithms or color image models could be considered. This work introduces a new color image component controlling image enhancement framework. This framework is illustrated on enhancement of low exposure underwater images, by applying a commonly used histogram equalization method on only one grayscale image that represents the color image in grays. The ratios of colors are preserved at each pixel, and in general, we assume that some changes of these ratios might also be considered, by introducing special functions on ratios; but this topic is beyond the score of our paper.

B. Quantitative Measure of Color Image Enhancement

To measure the quality of color images, we consider the described in [38,39],[58]-[60] quantitative measure of image enhancement that is based on the ratio of the maximum and minimum of intensity in the logarithm scale. This measure is based on the Weber and Fechner laws stated that the human visual detection depends not on the difference but the ratio of light intensity [36]. A grayscale discrete image $\{x_{n,m}\}$ of size $N_1 \times N_2$ is divided by $k_1 k_2$ blocks of given size $L_1 \times L_2$ each, where integers $k_i = \lfloor N_i/L_i \rfloor$, $i = 1,2$. Here, the rounding operation is denoted by $\lfloor . \rfloor$. The quantitative measure of enhancement of the image is calculated by

$$EME(x) = \frac{1}{k_1 k_2} \sum_{k=1}^{k_1} \sum_{l=1}^{k_2} 20 \ln \left[\frac{\max_{k,l}(x)}{\min_{k,l}(x)} \right]. \qquad (12)$$

$\max_{k,l}(x)$ and $\min_{k,l}(x)$ respectively are the maximum and minimum of the image $f_{n,m}$ inside the (k,l)-th block. In this block, the ratio in the logarithm

$$\mathrm{r}_{k,l} = \ln \left[\frac{\max_{k,l}(x)}{\min_{k,l}(x)} \right] = \ln \left(\max_{k,l}(x) \right) - \ln \left(\min_{k,l}(x) \right)$$

shows the range of intensity of the image in the logarithm scale. Therefore, $EME(x)$ determines the average-block scale of intensities in the image. For many images, the 5×5 or 7×7 blocks are used, when calculating the measure EME. In calculation of the EME function, the blocks with zero $\min_{k,l}(x)$ can be skipped or the number 1 can be added to the image x, to avoid zero values of x for $\ln(x)$ function. For images with a noise, instead of maximum and minimum operations, we can consider the order statistics next to them. The quantitative measure of enhancement of the image can be defined by

$$EME(x) = \frac{1}{k_1 k_2} \sum_{k=1}^{k_1} \sum_{l=1}^{k_2} 20 \ln \left[\frac{(\mathrm{OR}_2)_{k,l}(x)}{(\mathrm{OR}_{\mathrm{T}-1})_{k,l}(x)} \right], \qquad (13)$$

where $T = k_1 k_2$, and $(\mathrm{OR}_2)_{k,l}(x)$ and $(\mathrm{OR}_{\mathrm{T}-1})_{k,l}(x)$ are the order statistic number 2 and $T-1$, respectively, of the image $x_{n,m}$ inside the (k,l)-th block.

When processing color images $f = (r,g,b)$ in the RGB color model, we can analyze the enhancement functions EME for all three channels. However, as shown in [57,58], instead of calculating three functions $EME(r)$, $EME(g)$, and $EME(b)$, the following enhancement measure [61] of the color image can be used:

$$EMEC(f) = \frac{1}{k_1 k_2} \sum_{k=1}^{k_1} \sum_{l=1}^{k_2} 20 \ln \left[\frac{\max_{k,l}(r,g,b)}{\min_{k,l}(r,g,b)} \right]. \qquad (14)$$

Thus, the maximum and minimum values of the color image in the (k,l)-th block are calculated as $\max(f) = \max(r,g,b)$ and $\min(f) = \min(r,g,b)$. This concept of enhancement measure, EMEC, was used when processing the image by the traditional 2-D DFT, as well as by the quaternion 2-D DFT [47],[50]-[52]. The color enhancement measure EMEC can be used to estimate enhancement in the RGB color space and other color models. In the XYZ space, when $f = (f_X, f_Y, f_Z)$, the enhancement measure is similarly defined:

$$EMEC(f) = \frac{1}{k_1 k_2} \sum_{k=1}^{k_1} \sum_{l=1}^{k_2} 20 \ln \left[\frac{\max_{k,l}(f_X, f_Y, f_Z)}{\min_{k,l}(f_X, f_Y, f_Z)} \right].$$

III. Experimentary Results

In this section, we illustrate the color histogram equalization (CHE) in the proposed model. The results of CHE are given together with the HE applied separately for each color component. As an example, we consider the underwater color "fishes" image of size 601×980 that is shown in Fig. 3. The EMEC of this image is 20.81 with the block size $L_1 \times L_2 = 5 \times 5$. All EMEC and EME measures calculated on color and grayscale images in this paper use the same block size 5×5.

 ISSN: 2454-4248
36 – 47

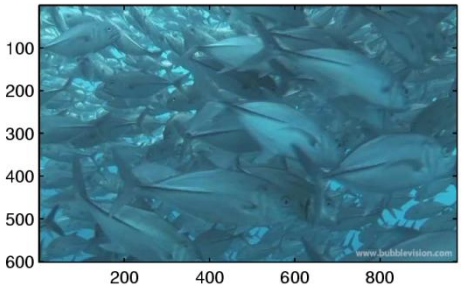

Figure 3. Original color image in the RGB model.

When transferring this color image $f_{n,m}$ into a grayscale image, in Step 2 of the diagram in Fig. 2, we consider the case when $a_1 = a_2 = 1/3$, and

$$i_{n,m} = (r_{n,m} + g_{n,m} + b_{n,m})/3, \quad (15)$$

where $n = 0{:}600$ and $m = 0{:}979$. Figure 4 shows this grayscale image for the "fishes" image. The EME of this grayscale image is 2.79.

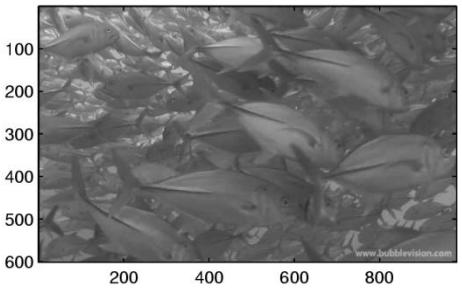

Figure 4. The grayscale image representing the color "fishes" image.

On this stage of the algorithms, the ratios of colors $\lambda_1(n,m)$ and $\lambda_2(n,m)$ that are described in Eqs. 4 and 5 are calculated. Figure 5 shows the ratio $\lambda_1(n,m)$ as the grayscale image.

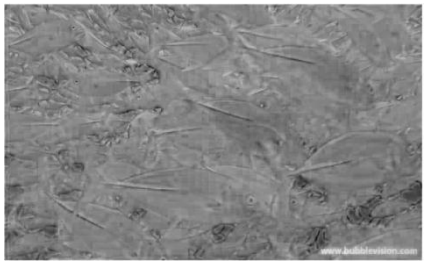

Figure 5. The grayscale image representing the ratio $\lambda_1(n,m)$ for the color "fishes" image.

The histogram equalization of the grayscale "fishes" image $i_{n,m}$ is shown in Fig. 6. The EME of the new image $i'_{n,m}$ is parts (a), (b), and (d), respectively. The EMEC of the new color image is 12.55, which is larger than for the original grayscale image, $EME(i) = 2.79$.

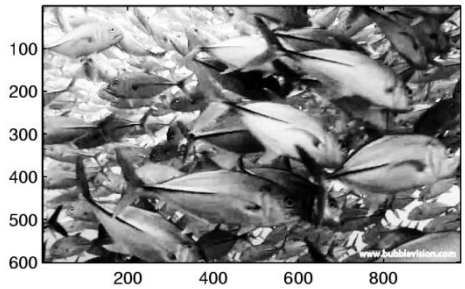

Figure 6. The histogram equalization of the grayscale image $i_{n,m}$.

Figure 7 shows the histogram of the grayscale "fishes" image $i_{n,m}$ before and after the histogram equalization in parts (a) and (b), respectively.

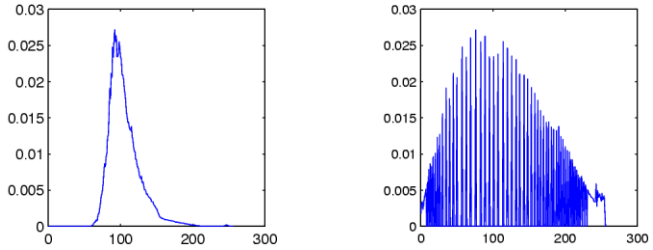

(a) (b)

Figure 7. Histograms of (a) the grayscale image and (b) of its HE.

The new color image is "reconstructed" by Eq. 8 from the obtained grayscale image, by using the calculated ratios of colors, as described in Step 5 in the above block-diagram. Since, $a_1 = a_2 = 1/3$, the sum of new colors $s'_{n,m} = 3i'_{n,m}$. Figure 8 shows the new color image $f'_{n,m}$ in part (c). The histograms of new red, green, and blue colors are shown in parts (a), (b), and (d), respectively. The EMEC of the new color image is 29.11, i.e., the improvement in measure is equal to $EMEC(f'_{n,m}) - EMEC(f_{n,m}) = 29.11 - 20.81 = 8.30$.

As can be seen from the above histograms, the ranges of the green and blue components of the image exceed the original range [0, 255]. Therefore, we can scale the color components into this range and obtain the image that is shown in Fig. 9 in part (b). This procedure reduces the EMEC of the CHE of this image to 22.56.

A. HE of All Color Components

In this subsection, we illustrate a few results of color image enhancement with the traditional approach when each color component of the "fishes" and other images are processed separately.

Figure 10 shows the grayscale transformation of the HE of color components of the "fishes" image. The values of EME measure for each of three color components before and after the HE are given in Table 1. One can see the increase in measure for all three components. For instance, the EME of the color component from $EME(r_{n,m}) = 4.96$ increases more than tree times to $EME(r'_{n,m}) = 16.60$.

 ISSN: 2454-4248
36 – 47

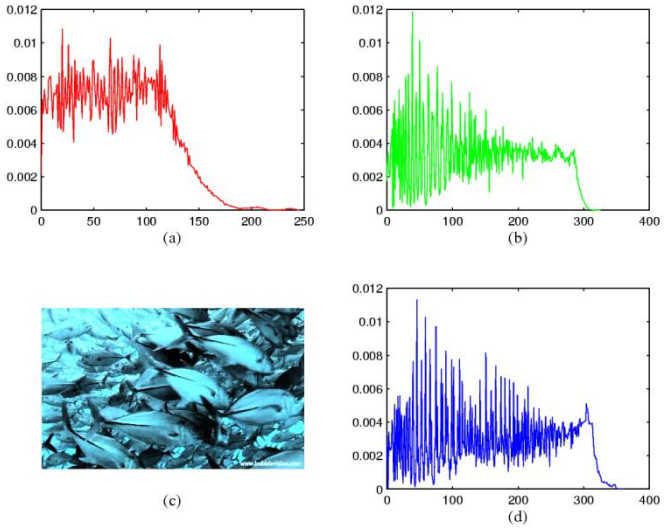

Figure 8. Histograms of the (a,b,d) red, green, and blue components of the (c) new color image.

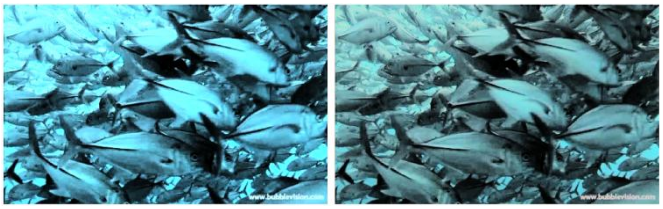

(a) (b)

Figure 9. The CHE of the "fishes" image (a) before and (b) after scaling the range of colors (with EMEC equal 29.81 and 22.56, respectively).

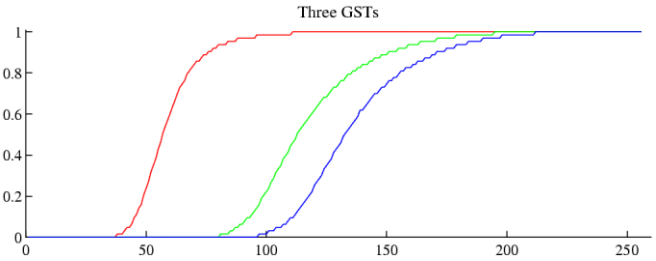

Figure 10. Three grayscale transformations of colors in component-wise HE.

Figure 11 shows the result of the component-wise HE of the "fishes" image in part (a) and the result of the CHE in part (b).

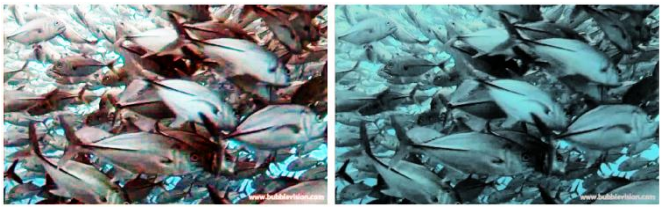

(a) (b)

Figure 11. The HE of the image applied separately three times to color components and (b) only ones in the proposed model.

The enhancement measure of the component-wise HE of the "fishes" image is 20.42 that is less than the EME of the CHE, as shown in Table 1.

image	EME	New EME	EMEC
Original color			20.81
Red	4.96	16.10	
Green	2.60	10.84	
Blue	2.28	10.42	
HE by 3 colors			20.42
Color HE			29.11
Color HE (scaled)			22.56

Table 1: Measures of images by the color-wise HE and CHE.

In another example, Fig. 12 shows the color image (which we call the "big fish" image) of size 340×561 in part (a) and the result of the component-wise HE of the image in part (b). The image has been enhanced; however, the colors of the ground and pebble on it can actually not be the colors of "the sunny coast" under the water, as they are seen in the image in part (b).

(a) (b)

Figure 12. (a) The color image and (b) HE of the image applied separately three times for color components.

We consider the application of the CHE. Figure 13 shows the CHE when preserving the color ratios the in part (a). The scaled version of this image is given in part (b).

(a) (b)

Figure 13. The color HE of the image (a) before and (b) after the scaling the range of colors to [0, 255].

EMEC measures of these images are given in Table 2.

 ISSN: 2454-4248
36 – 47

Color image	Measure EMEC
"big fish"	29.5971
HE by 3 colors	32.9611
color HE	40.6279
color HE (scaled)	42.1228

Table 2: Measures of images by the color-wise HE and CHE.

It should be noted that our main goal is not to compare the results of CHE in the proposed and traditional models of color imaging. The goal is to show that the proposed model can be used together with the traditional model in color image enhancement.

In another example, Fig. 14 shows the color "coral" image of size 405×763 in part (a) and the result of the component wise HE of the image in part (b).

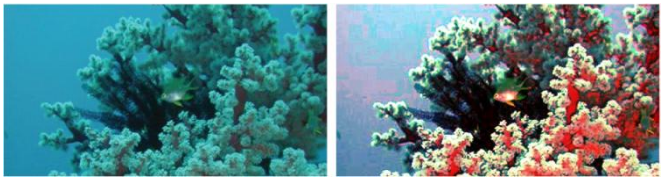

(a) (b)

Figure 14. (a) The color "coral" image and (b) HE of the image applied separately three times for color components.

Figure 15 shows the CHE when preserving the color ratios in part (a). The scaled version of this image is given in part (b).

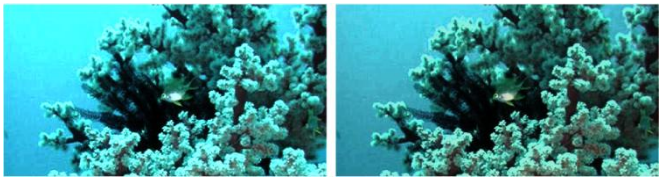

(a) (b)

Figure 15. The CHE of the "coral" image (a) before and (b) after the scaling the range of colors to [0, 255].

The values of EMEC measure of these images are given in Table 3.

Color image	Measure EMEC
"coral"	34.5695
HE by 3 colors	23.1553
color HE	37.3534
color HE (scaled)	33.3087

Table 3: Measures of images by the color-wise HE and CHE.

In Fig. 16, the color image (which we call the "fish #2" image) of size 350×525 is shown in part (a), and the CHE of the image in parts (b) and (c). The values of EMEC measure of these images are given in Table 4.

(a) (b) (c)

Figure 16. (a) The color image and the CHE preserving the color ratios (b) before and (c) after the scaling.

Color image	Measure EMEC
"fish #2"	9.1181
color HE	13.2459
color HE (scaled)	14.2745

Table 4: Measures of images by the CHE.

Figure 17 shows the color image of size 1843×1230 in part (a). The image enhanced by the CHE is shown in part (b) and its scaled version in part (c).

(a) (b) (c)

Figure 17. (a) The original image in the RGB color model (EMEC is 19.0563) and CHE (b) before (EMEC is 30.2193) and (c) after scaling (EMEC is 21.4421).

The CHE is calculated from the HE of the grayscale image that is shown in Fig. 18 in part (a). The EME measure of this image is 2.0866 and the EME=7.2171 is for the HE that is shown in part (b).

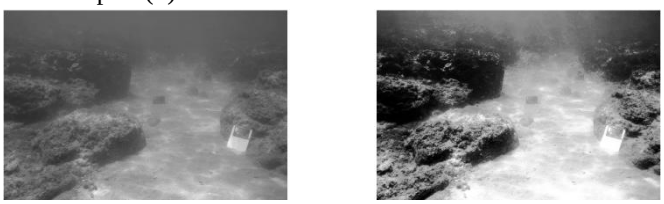

(a) (b)

Figure 18. (a) The grayscale image (EME is 2.0866) and (b) the HE of the image (EME is 7.2171).

Figure 19 shows the color image of size 1496×2000 of the AirAsia 8501 plane's part found underwater. The result of the HE that was applied separately three times for color components of the image is shown in part (b). The CHE of the color image, which was applied in the proposed model, is shown in part (c).

 ISSN: 2454-4248
36 – 47

(a) (b) (c)

Figure 19. (a) The color image, (b) the HE applied separately to each color components, and (c) the CHE preserving the color ratios.

EMEC measures of these images are given in Table 5.

Color image	Measure EMEC
"AirAsia 8501"	9.2349
HE of 3 colors	9.2270
color HE	10.5884

Table 5: Measures of images enhanced by the histogram equalization.

It should be noted that the color images $f_{n,m}$ can also be enhanced though processing their "negative" images $x_{n,m} = 255 - f_{n,m}$, by the following diagram:

$$f_{n,m} \to x_{n,m} \to x'_{n,m} = \mathrm{CHE}[x_{n,m}] \to f'_{n,m} \to 255 - x'_{n,m}.$$

Thus, the CHE is calculated on the "negative" color image and, then, the second "negative" image is calculated.

Figure 20 illustrates the results of the CHE that was applied on the "negative" of the "AirAsia 8501" image that is shown in Fig. 19(a). The EMEC value of the processed image by this CHE is 18.6966 and 13.3442 after the scaling.

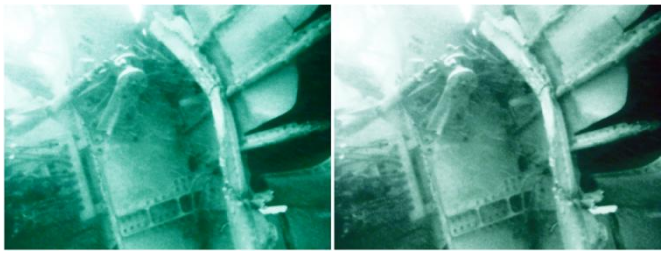

(a) (b)

Figure 20. CHE of the "AirAsia 8501" image (a) before and (b) after the scaling.

In the proposed model, the method of histogram equalization can be used together with the alpha-rooting enhancement, to increase the contrast and make more visible many details of the image after equalization. As example, Fig. 21 shows the grayscale image in part (a), which is calculated from the color image shown in Fig. 1(a). The HE of the grayscale image is shown in part (b) and after 0.94-rooting in part (c). This value of is chosen from the maximum of the measure function $EME(\alpha)$ calculated for different values of α from (0.5,1].

(a) (b) (c)

Figure 21. (a) The grayscale image (EME=1.7572), (b) the HE of the image (EME=8.7551), and (b) α-rooting of the HE (EME=11.2236).

The color HE of these images is illustrated in Fig. 22. The image enhanced by the CHE, when using the grayscale image of HE, is shown in part (a) and in part (c) after scaling. The image enhanced by the CHE, when using the α-rooting of the HE, is shown in part (b) and in part (d) after scaling.

(a) (b) (c) (d)

Figure 22. The color image enhancement, when using (a) the grayscale image, (b) the 0.94-rooting of the grayscale image, and (c) the image in (a) after scaling, (d) the image in (b) after scaling.

IV. Color Bi-Histogram Equalization

It is known that the histogram equalization does not preserve the mean value of the image. In the method of bi-histogram equalization (bi-HE), this property can be achieved by dividing the range of intensity $[r_0, r_1]$ by three parts $[r_0, t_1]$, (t_1, t_2), and $[t_2, r_1]$ with two thresholds t_1 and t_2, such that $r_0 < t_1 < t_2 \le r_1$. The HE separately is applied for the first two parts; the intensities greater than r are not changed. Such bi-HE is described by the transform

$$B(r) = \begin{cases} r_0 + (t_1 - r_0)F(r), & \text{if } r \in [r_0, t_1]; \\ t_1 + 1 + (t_2 - t_1 - 1)[F(r) - F(t_1)], & \text{if } r \in (t_1, t_2]; \\ r, & \text{if } r \in (t_2, r_1]. \end{cases}$$

The values of the thresholds t_1 and t_2 are selected by the user, as well as by the methods proposed by Otsu [75] or the method of EME [76]. In the $t_2 = r_1$ case, when the intensity range is divided by two parts, $[r_0, t_1]$ and $(t_1, r_1]$, the bi-HE is described by the transform

$$B(r) = \begin{cases} r_0 + (t_1 - r_0)F(r), & \text{if } r \in [r_0, t_1]; \\ t_1 + 1 + (t_2 - t_1 - 1)[F(r) - F(t_1)], & \text{if } r \in (t_1, r_1]. \end{cases}$$

The processing of the color image in the proposed model with the bi-HE can be named *the color bi-HE*.

As an example, Fig. 23(a) shows the histogram of the grayscale image presenting the color image of the "fish" image shown in Fig. 12(a). This grayscale image was calculated by Eq. 2. The threshold $t_1 = 40$ is also shown with the histogram. The result of the bi-HE of the grayscale image is shown in Fig. 23(b) and the histogram of the new image in Fig. 23(c).

 ISSN: 2454-4248
36 – 47

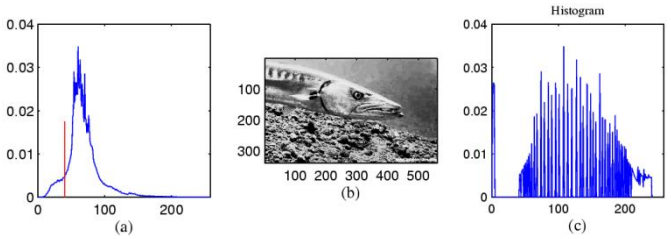

Figure 23. (a) The histogram of the grayscale "big fish" image, (b) bi-HE of the image, and (c) histogram of the bi-HE.

In the proposed model, from this grayscale image the color image is calculated by using the rations of colors of the original "big fish" image. Figure 24 shows the original "big fish' image in part (a) and the color image reconstructed from the bi-HE of the grayscale image in part (b). This bi-CHE of the image has the measure EMEC equal to 45.0517, or 46.0656 after the scaling, which are larger than the corresponding values that are given in Table 2 for the CHE.

(a) (b)

Figure 24. (a) The 'big fish' color image and (b) the bi-CHE of this image.

We also consider the color image that is shown in Figure 16(a), which we name the "small fish." The grayscale image calculated from this color image is shown in Fig. 25 in part (a) and its histogram in part (c). Two thresholds, $t_1 = 80$ and $t_2 = 140$, are selected. The result of processing this image by the bi-HE with these thresholds is shown in part (b) and its histogram in part (d). These two thresholds are taken from the bright range intensity with very small values of histogram.

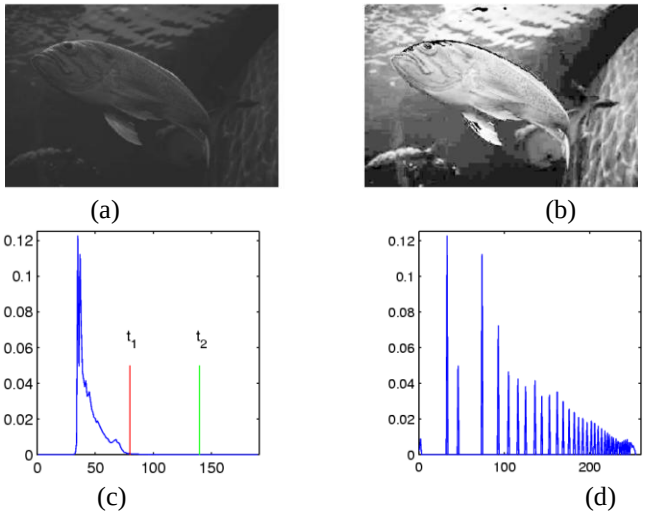

Figure 25. (a) The color "small fish" image and (b) the bi-HE with the threshold 40, and (c) and (d) histograms of these images, respectively.

In the proposed model, the color image was calculated from the grayscale image of the bi-HE, by using the rations of colors of the original image. Figure 26 shows the original "small fish' image in part (a) and the color image reconstructed from the bi-HE of the grayscale image in part (b). One can note a good enhancement of the image.

(a) (b)

Figure 26. (a) The color "small fish" image and (b) color bi-HE of this image.

V. CONCLUSION

The new model for processing color images is proposed, which is based on the idea of preserving the color ratios in the image and processing the image in grays. The examples of color image enhancement by the histogram equalization are given together with the separate enhancement by all color components. The proposed model with color ratios can be used not only for the HE equalization. In the block #4 of the block diagram in Fig. 2, the bi-HE and many grayscale transformations different from HE can be applied, too. For instance, we consider the square-root transformation $x \to 16\sqrt{x+1}$, when the range of the image is [0,255]. As an example, Fig. 27 shows the original color image of size 350×400 in part (a) and the square-root transform applied in the proposed model with color ratios in part (b). This model can also be used when enhancing color images in the frequency domain, for instance by the alpha-rooting, zonal alpha-rooting, and retinex.

(a) (b)

Figure 27. (a) The color image and (b) the square-root transform preserving the color ratios.

REFERENCES

[1] L. Wang, Q. Dai, Q. Xu, Y. Zhang, "Constructing Hierarchical Segmentation Tree for Feature Extraction and Land Cover Classification of High Resolution MS Imagery," Selected Topics in Applied Earth Observations and Remote Sensing IEEE Journal of, 2015, vol. 8, pp. 1946-1961.

[2] F. Isikdogan, A. Bovik, P. Passalacqua, "Surface water mapping by deep learning," IEEE Journal of Selected Topics in Applied Earth Observations and Remote Sensing, 2017, vol. 10, no. 11.

[3] X. Zhang, P. Xiao, X. Feng, L. Feng, N. Ye, "Toward evaluating multiscale segmentations of high spatial resolution remote sensing Images," Geoscience and Remote Sensing IEEE Transactions on, 2015, vol. 53, pp. 3694-3706.

[4] F. Xie, M. Shi, Z. Shi, J. Yin, D. Zhao, "Multilevel Cloud Detection in Remote Sensing Images Based on Deep Learning," IEEE Journal of Selected Topics in Applied Earth Observations and Remote Sensing, 2017, vol. 10, no. 8, pp. 3631-3640.

[5] G.J. Jedlovec, S.L. Haines, F.J. LaFontaine, "Spatial and temporal varying thresholds for cloud detection in goes imagery", IEEE Trans. Geosci. Remote Sens., 2008, vol. 46, no. 6, pp. 1705–1717.

[6] Y. Yuan, X. Hu, "Bag-of-words and object-based classification for cloud extraction from satellite imagery", IEEE Journal of Selected Topics in Applied Earth Observations and Remote Sensing, 2015, vol. 8, no. 8, pp. 4197–4205.

[7] R. Shang, Y. Yuan, L. Jiao, B. Hou, A.M.G. Esfahani, R. Stolkin, "A fast algorithm for SAR image segmentation based on key pixels," IEEE Journal of Selected Topics in Applied Earth Observations and Remote Sensing, 2017, vol. 10, no. 12.

[8] G.D. Martins, B.T. Galo, B.S. Vieira, "Detecting and mapping root-knot nematode infection in coffee crop using remote sensing measurements," 2017, pp. 5395–5403.

[9] J. Ning, R. Wang, Y. Deng, N. Li, H. Song, W. Fei, A Novel Approach to Enhance Azimuth Resolution for ScanSAR Interferometry, AET-IAA, 2017, pp. 5674–5685.

[10] J. Y. Chiang, Y.-C. Chen, "Underwater image enhancement by wavelength compensation and dehazing," IEEE Trans. on Image Processing, 2012, vol. 21, no. 4, pp. 1756–1769.

[11] S. Raimondo, C. Silvia, "Underwater image processing: State of the art of restoration and image enhancement methods," EURASIP J.Adv. Signal Processing, 2010, vol. 2010.

[12] K. Panetta, C. Gao, S. Agaian, "Human-visual-system-inspired underwater image quality measures," IEEE Journal of Oceanic Engineering, 2016, vol. 41, no. 3.

[13] B.A. McGlamery, "Computer model for underwater camera system," Proc. of SPIE, 1979, vol. 208, pp. 221–231.

[14] H. Lu, Y. Li, S. Serikawa, "Computer vision for ocean observing," Artificial Intelligence and Computer Vision, 2016, pp. 1–16.

[15] F. Bonin, A. Burgeara, "Imaging system for advanced underwater vehicles," Journal of Maritime Research, 2011, vol. 8, no. 1, pp. 65-86.

[16] R. Schettini, S. Corchs, "Underwater image processing: state of the art of restoration and image enhancement methods," EURASIP J. Adv. Signal Process, 2010.

[17] M. Ludvigsen, B. Sortland, G. Johnsen, S. Hanumant, "Applications of geo-referenced underwater phot o mosaics in marine biology and archaeology," J. Oceanography, 2007, vol. 20, no. 4, pp. 140–149.

[18] N.J.C. Strachan, "Recognition of fish species by colour and shape," J. Image Vis. Comput., 1993, vol. 11, no. 1, pp. 2–10.

[19] L.A. Torres-Mndez, G. Dudek, "Color correction of underwater images for aquatic robot inspection," Proc. EMMCVPR, 2005, pp. 60–73.

[20] C.-Y. Li, Ji-C. Guo, R.-M. Cong, Yan-Wei Pang, "Underwater image enhancement by dehazingwith minimum information loss and histogram distribution prior," IEEE Trans. on Image Processing, 2016, vol. 25, no. 12.

[21] K. Zuiderveld, "Contrast limited adaptive histogram equalization," Graphics Gems IV, San Diego, CA, USA: Academic, 1994, pp. 474–485.

[22] G. Deng, "A generalized unsharp masking algorithm," IEEE Trans. on Image Processing, 2011, vol. 20, no. 5, pp. 1249–1261.

[23] X. Fu, Y. Liao, D. Zeng, Y. Huang, X. P. Zhang, X. Ding, "A probabilistic method for image enhancement with simultaneous illumination and reflectance estimation," IEEE Trans. Image Proc., 2015, vol. 24, no. 12, pp. 4965–4977.

[24] S.C. Nercessian, K.A. Panetta, S.S. Agaian, "Non-linear direct multiscale image enhancement based on the luminance and contrast masking characteristics of the human visual system," IEEE Trans. on Image Proc., 2013, vol. 22, no. 9, 2549-2561.

[25] E. Wharton, S. Agaian, K. Panetta, "Adaptive multi-histogram equalization using human vision thresholding," Proc. SPIE, 2007, vol. 6497, p. 64970G.

[26] E. Wharton, K. Panetta, S. Agaian, "Human visual system based multi-histogram equalization for non-uniform illumination and shadow correction," Proc. IEEE Int. Conf., 2007, vol. 1, pp. 729–732.

[27] L. Lu, Y. Zhou, K. Panetta, S. Agaian, "Comparative study of histogram equalization algorithms for image enhancement," Proc. SPIE, 2010, vol. 7708, pp. 770811-1–770811-11.

[28] R.C. Gonzalez, R.E. Woods, Digital Image Processing, 2nd Edition, Prentice Hall, 2002.

[29] A.M. Grigoryan, S.S. Agaian, "Monotonic sequences for image enhancement and segmentation," Digital Signal Processing, 2015, vol. 41, pp. 70-89, (doi:10.1016/j.dsp.2015.02.011).

[30] A.M. Grigoryan, S.S. Agaian, "Preprocessing Tools for Computer-Aided Cancer Imaging Systems," book-chapter 2 in "Computer-Aided Cancer Detection and Diagnosis: Recent Advances" (Editors: J. Tang, S. Agaian), SPIE, 2014, pp. 23-78.

[31] W.M. Morrow, R.B. Paranjape, R.M. Rangayyan, J.E.L. Desautels, "Region-based contrast enhancement of mammograms," IEEE Trans. on Medical Imaging, 1992, vol. 11, no. 3, pp. 392–406.

[32] T.L. Ji, M.K. Sundareshan, H. Roehrig, "Adaptive image contrast enhancement based on human visual properties," IEEE Trans. on Medical Imaging, 1994, vol. 13, no. 4, pp. 573–586.

[33] J.H. McClellan, "Artifacts in alpha-rooting of images," Proc. IEEE Int. Conf. Acoustics, Speech, and Signal Processing, 1980, pp. 449-452.

[34] H. J. Trussell, E. Saber, M. Vrhel, "Color image processing," IEEE Signal Processing Mag., 2005, vol. 22, no. 1, pp. 14-22.

[35] A. Tremeau, S. Tominaga, K.N. Plataniotis, "Color in image and video processing: Most recent trends and future research

directions," EURASIP Journal on Image and Video Processing, 2008, vol. 2008, 26 p.

[36] S. Hecht, "The visual discrimination of intensity and the Weber-Fechner law," The Journal of General Physiology, 1924, pp. 235-267.

[37] A.M. Grigoryan, Multidimensional Discrete Unitary Transforms. In the Third Edition Transforms and Applications Handbook in The Electrical Engineering Handbook Series (Editor in Chief, A. Poularikas). CRC Press Taylor and Francis Group, 2010.

[38] A.M. Grigoryan, S.S. Agaian, Multidimensional Discrete Unitary Transforms: Representation, Partitioning and Algorithms, Marcel Dekker Inc., New York, 2003.

[39] A.M. Grigoryan, M.M. Grigoryan, Brief Notes in Advanced DSP: Fourier Analysis With MATLAB, CRC Press Taylor and Francis Group, 2009.

[40] S.S. Agaian, H.G. Sarukhanyan, K.O. Egiazarian, J. Astola, "Hadamard Transforms," SPIE Press, 2011.

[41] A.M. Grigoryan, M. Hajinoroozi, "A novel method of filtration by the discrete heap transforms, [9019-2], SPIE proceedings, 2014 Electronic Imaging: Image Processing: Algorithms and Systems XII, February 2-6, San Francisco, California, 2014.

[42] A.M. Grigoryan, M. Hajinoroozi, "Image and audio signal filtration with discrete Heap transforms," Applied Mathematics and Sciences: An Int. Journal, 2014, vol. 1, no. 1, pp. 1–18.

[43] K. Naghdali, R. Ranjith, A. Grigoryan, "Fast signal-induced transforms in image enhancement," Proc. Systems, Man and Cybernetics, SMC 2009, IEEE Int. Conference on, pp. 565-570.

[44] A.M. Grigoryan, S.P.K. Devieni, "New method of signal denoising by the paired transform," Applied Mathematics and Sciences: An International Journal, 2014, vol. 1, no. 2, pp. 1–20.

[45] A.M. Grigoryan, S.S. Agaian, "Alpha-rooting method of color image enhancement by discrete quaternion Fourier transform," [9019-3], SPIE proceedings, 2014 Electronic Imaging: Image Processing: Algorithms and Systems XII, 2014, p. 12.

[46] A.M. Grigoryan, S.S. Agaian, "Retooling of color imaging in the quaternion algebra," Applied Mathematics and Sciences: An International Journal (MathSJ), 2014, vol. 1, no. 3, pp. 23–39.

[47] A.M. Grigoryan, J. Jenkinson, S.S. Agaian, "Quaternion Fourier transform based alpha-rooting method for color image measurement and enhancement," SIGPRO-D-14-01083R1, Signal Processing, 2015, vol. 109, pp. 269–289.

[48] A.M. Grigoryan, S.S. Agaian, "2-D Left-side quaternion discrete Fourier transform fast algorithms," Proc. IS&T International Symposium, 2016 Electronic Imaging: Algorithms and Systems XIV, February 14-18, San Francisco, California, 2016.

[49] A.M. Grigoryan, S.S. Agaian, "Tensor transform-based quaternion Fourier transform algorithm," Information Sciences, 2015, vol. 320, pp. 62–74.

[50] A.M. Grigoryan, S.S. Agaian, "Color enhancement and correction for camera cell phone medical images using quaternion tools," in Electronic Imaging Applications in Mobile Healthcare, J. Tang, S.S. Agaian, and J. Tan, Eds., SPIE Press, Bellingham, Washington, 2016, ch. 4, pp. 77–117.

[51] A.M. Grigoryan, S.S. Agaian, "Alpha-rooting method of gray-scale image enhancement in the quaternion frequency domain," Proc. IS&T International Symposium, Electronic Imaging: Algorithms and Systems XV, 2017.

[52] A.M. Grigoryan, A. John, S.S. Agaian, "Color image enhancement of medical images using alpha-rooting and zonal alpha-rooting methods on 2-D QDFT," Proceedings of SPIE Medical Imaging Symposium, Image Perception, Observer Performance, and Technology Assessment conference, 2017.

[53] A.M. Grigoryan, S.S. Agaian, "Tensor form of image representation: enhancement by image-signals," Proc. IS&T/SPIEs Symposium on Electronic Imaging Science & Technology, San Jose. CA, 2003, 12p.

[54] F.T. Arslan, A.M. Grigoryan, "Fast splitting alpha-rooting method of image enhancement: Tensor representation," IEEE Trans. on Image Proc. 2006, vol. 15, no. 11, pp. 3375–3384.

[55] A.M. Grigoryan, N. Du, "2-D images in frequency-time representation: Direction images and resolution map," Journal of Electronic Imaging, 2010, vol. 19, no. 3, p. 033012.

[56] A.M. Grigoryan, N. Du, "Principle of superposition by direction images," IEEE Trans. on Image Processing, 2011, vol. 20, no. 9, pp. 2531–2541.

[57] A.M. Grigoryan, K. Naghdali, "On a method of paired representation: Enhancement and decomposition by series direction images," Journal of Mathematical Imaging and Vision, 2009, vol. 34, no. 2, pp. 185–199.

[58] S.S. Agaian, K. Panetta, A.M. Grigoryan, "A new measure of image enhancement, Proc. of the IASTED Int. Conf. Signal Processing Communication, Marbella, Spain, Sep. 19-22, 2000.

[59] S.S. Agaian, K. Panetta, A.M. Grigoryan, "Transform-based image enhancement algorithms," IEEE Trans. on Image Processing, 2001, vol. 10, no. 3, pp. 367–382.

[60] A.M. Grigoryan, S.S. Agaian, "Transform-based image enhancement algorithms with performance measure," Advances in Imaging and Electron Physics, Academic Press, 2004, vol. 130, pp. 165–242.

[61] Z. Rahman, D. Jobson,G.A. Woodell, "Retinex processing for automatic image enhancement," Journal of Electronic Imaging, 2004, vol. 13, no. 1, pp. 100–110.

[62] K.-Q. Huang, Q. Wang, Z.-Y. Wu, "Natural color image enhancement and evaluation algorithm based on human visual system," Computer Vision and Image Understanding, 2006, vol. 103, no. 1, pp. 52-63.

[63] D.J. Jabson, Z.Rahman, G.A. Woodell, "A multi-scale retinex for bridging the gap between color images and the human observation of scenes," IEEE Trans. on Image Proc.: Special Issue on Color Processing, 1997, vol. 6, no. 7, pp. 965–976.

[64] A.M. Gonzales, A.M. Grigoryan, "Fast Retinex for color image enhancement: Methods and algorithms," Proc. SPIE, Electronic Imaging: Mobile Devices and Multimedia: Enabling Technologies, Algorithms, and Applications, 2015, vol. 9411, 12p.

[65] A.M. Grigoryan, S.S. Again, A.M. Gonzales, "Fast Fourier transformbased retinex and alpha-rooting color image enhancement," [9497-29], Proc. SPIE Conf., Mobile Multimedia/Image Processing, Security, and Applications, 2015, 12p.

[66] J. Mukherjee, S.K. Mitra, "Enhancement of color images by scaling the DCT coefficients," IEEE Trans. on Image Processing, 2008, vol. 17, no. 10, pp. 1783–1794.

[67] K. Panetta, J. Xia, S. Agaian, "Color image enhancement based on the discrete cosine transform coefficient histogram," Journal of Electronic Imaging, 2012, vol. 21, no. 2, pp. 1-17.

[68] K. Panetta, Y. Zhou, S. Agaian, H. Jia, "Nonlinear Unsharp Masking for Mammogram Enhancement," IEEE Trans. on Information Technology in Biomedicine, 2011, vol. 15, pp. 918-928.

[69] S.S. Agaian, B. Silver, K.A. Panetta, "Transform coefficient histogrambased image enhancement algorithms using contrast entropy," IEEE Trans. on Image Processing, 2007, vol. 16, no. 3, pp. 741-758.

[70] J. Xia, K.A. Panetta, S. Agaian, "Color image enhancement algorithm based on DCT transforms," Proceedings, Man and Cybernetics, SMC 2011. IEEE Inter. Conf., 2011, pp. 1496-1501.

[71] B. Silver, S.S. Agaian, K.A. Panetta, "Contrast entropy based image enhancement and logarithmic transform coefficient histogram shifting," Proceedings, IEEE ICASSP, March 2005.

[72] K. Panetta, C. Gao, S. Agaian, "No reference color image contrast and quality measures," IEEE Trans. on Consumer Electronics, 2013, vol. 59, no. 3, pp. 643-651.

[73] K. Panetta, S. Agaian, Z. Yicong, E.J. Wharton, Parameterized logarithmic framework for image enhancement systems,"Man, and Cybernetics, Part B: Cybernetics, IEEE Trans. on, 2011. vol. 41, no. 2, pp. 460–473.

[74] K. Panetta, E. Wharton, S. Agaian, "Human visual system based image enhancement and measure of image enhancement," IEEE Trans. on Systems, Man and Cybernetics-Part A: Systems and Humans, 2008, vol. 38, no. 1, pp. 174–188.

[75] N. Otsu, "A threshold selection method from gray-level histograms," IEEE Trans. on Systems, Man, and Cybernetics, 1979, vol. 9, no. 1, pp. 62–66.

[76] A.M. Grigoryan, S.S. Agaian, "Image Processing Contrast Enhancement," Wiley Encyclopedia of Electrical and Electronics Engineering, 22p, (2017). (doi: 10.1002/047134608X.W5525.pub2)

[77] C. Li, Ji. Guo, R. Cong, Y. Pang, B. Wang, "Underwater image enhancement by dehazing with minimum information loss and histogram," IEEE Trans. on Image Processing, 2016, vol. 25, no. 12, pp. 5664–5677.

[78] D. Berman, T. Treibitz, S. Avidan, "Diving into haze-lines: Color restoration of underwater images," Proc. British Machine Vision Conference (BMVC), 2017, 12p.

[79] A.M. Grigoryan, S.S. Agaian, Quaternion and Octonion Color Image Processing with MATLAB, SPIE, vol. PM279, [ISBN: 9781510611351], 2018, p. 404.

[80] A.M. Grigoryan, S.S. Agaian, "Color facial image representation with new quaternion gradients," Image Processing: Algorithms and Systems, IS&T Electronic Imaging Symposium, Burlingame, CA, 2018, 6p.

[81] A.M. Grigoryan, S.S. Agaian, "Color visibility images and measures of image enhancement," Proc. IS&T International Symposium, Electronic Imaging: Algorithms and Systems, Burlingame, CA, 2018, 5p.

[82] A.M. Grigoryan, A. John, S.S. Agaian, "Enhancement of underwater color images by two-side 2-D quaternion discrete Fourier transform," Proc. IS&T International Symposium, Electronic Imaging: Algorithms and Systems, Burlingame, CA, 2018, 6p.

[83] A.M. Grigoryan, A. John, S.S. Agaian, "Alpha-rooting color image enhancement method by two-side 2D-quaternion discrete Fourier transform followed by spatial transformation," International Journal of Applied Control, Electrical and Electronics Engineering, February 2018, vol. 6, no. 1, 21p.

[84] A.M. Grigoryan, S.S. Agaian, "Image enhancement by elliptic discrete Fourier transforms," International Journal on Future Revolution in Computer Science & Communication Engineering, 2018, vol. 4, no. 2, pp. 378 – 387.